



Microscopic theory of Raman scattering for the rotational organic cation in metal halide perovskites

Yu Cui, Yi-Yan Liu, Jia-Pei Deng, Xiao-Zhe Zhang, Ran-Bo Yang, Zhi-Qing Li, and Zi-Wu Wang ^{*}
 Tianjin Key Laboratory of Low Dimensional Materials Physics and Preparing Technology, Department of Physics,
 School of Science, Tianjin University, Tianjin 300354, China

 (Received 27 September 2022; revised 2 February 2023; accepted 6 March 2023; published 13 March 2023)

A gap exists in the microscopic understanding the dynamic properties of the rotational organic cation (ROC) in the inorganic framework of the metal halide perovskites (MHP) to date. Herein, we develop a microscopic theory of Raman scattering for the ROC in MHP based on the angular momentum of a ROC exchanging with that of the photon and phonon. We systematically present the selection rules for the angular momentum transfer among the three lowest rotational levels. We find that the phonon angular momentum that arises from the inorganic framework and its specific values could be directly manifested by Stokes (or anti-Stokes) shift. Moreover, the initial orientation of the ROC and its preferentially rotational directions could be judged in Raman spectra. This study lays the theoretical foundation for the high-precision resolution and manipulation of molecular rotation immersed in the many-body environment by Raman technique.

DOI: [10.1103/PhysRevB.107.094306](https://doi.org/10.1103/PhysRevB.107.094306)

I. INTRODUCTION

Over the past few years, metal halide perovskites (MHP) as promising materials have aroused intense interest from worldwide research owing to their notable properties, such as their ferroelectric property, long carrier lifetime, and high defect tolerance in the fields of photovoltaic cells, light-emitting diodes, and photodetectors [1–3]. Traditionally, the consensus is that the species of organic cations are not directly involved in the formation of electronic transport levels [4,5]. However, recent breakthroughs, studied by the spectral measurements [6–8] and first-principles calculation [9–12], showed that the dipole nature of the organic cation plays a critical role in the structure stabilizations and optoelectronic properties of MHP [13], e.g., the compositional engineering of organic cations to modulate the band gap and to modify the crystal symmetry and phase. In particular, the rotational motion of organic cation results in (1) ferroelectric domains controlling the ferroelectric polarization of perovskites [14–18] and (2) an effective Coulomb screening to affect the dynamics of charge carriers [12,13,19–21]. Therefore, the manipulation of the rotational organic cation (ROC) not only gives an effective method to modify the properties of MHP, but provides a test bed to explore novel quantum phenomena in many-body physics [13,22].

Based on the angular momentum exchange between photon and rotational particles, quantum control of the rotational atoms or molecules by laser were studied both theoretically and experimentally in areas of atomic, molecular, and optical physics as well as in physical chemistry [22–25], while the corresponding studies on ROC in perovskite materials are still very few. However, ROC inevitably couples with the surrounding inorganic cage [see Fig. 1(a)]. Although the coupling effect of the organic cation with the inorganic sublattice by hydrogen bonds were analyzed widely [26,27], the role of phonons of inorganic cage on the rotational dynamics of

the organic cation received relatively little attention, partially because of the intricate angular-momentum algebra from the ROC coupled with the many-body environment. Fortunately, Schmidt and Lemesko undertook a critical step towards such a theory in 2015 by introducing the quasiparticle concept of the “*angulon*”—a quantum rotor dressed by a bath of harmonic oscillators [28], which provided a simple and effective model to study the angular momentum exchange between the rotational molecule and many-body environment, such as molecules rotating in superfluid helium and ultracold alkali dimers interacting with a Bose-Einstein condensate [29,30]. However, to the best of our knowledge, the theoretical model for the angular momentum of ROC exchanges with both the photon and phonon in MHP has not yet been developed.

In this paper, we study the microscopic processes of Raman scattering mediated by a ROC in MHP based on ROC coupling with the photon and phonon. We present the selection rules of quantum transitions among the rotational eigenstates $|L, M\rangle$ of ROC (L and M denote the orbital angular quantum number and its projection on the laboratory-frame z -axis, respectively), in which the transitions from $L = l$ to $L = l'$ accompanying with and without the variation of the projection of angular quantum number are analyzed. We illustrate the Stokes and anti-Stokes shifting of Raman spectra for the three lowest rotational levels according to the different angular momenta provided by phonons. These results show that the transfer of phonon angular momentum, the initial orientation, and the magnitude of the rotational angle of a ROC could be reflected by Raman scattering, both of which are key problems for accurate quantum control of the ROC or molecules. More importantly, this model can be expanded to study molecules rotating in varieties of the cage-like structures, such as fullerene, the carbon nanotube, and so on.

II. THEORETICAL MODEL

In the frame of the classical model of Raman scattering mediated by elementary excitation, e.g., the electron and

^{*}wangziwu@tju.edu.cn

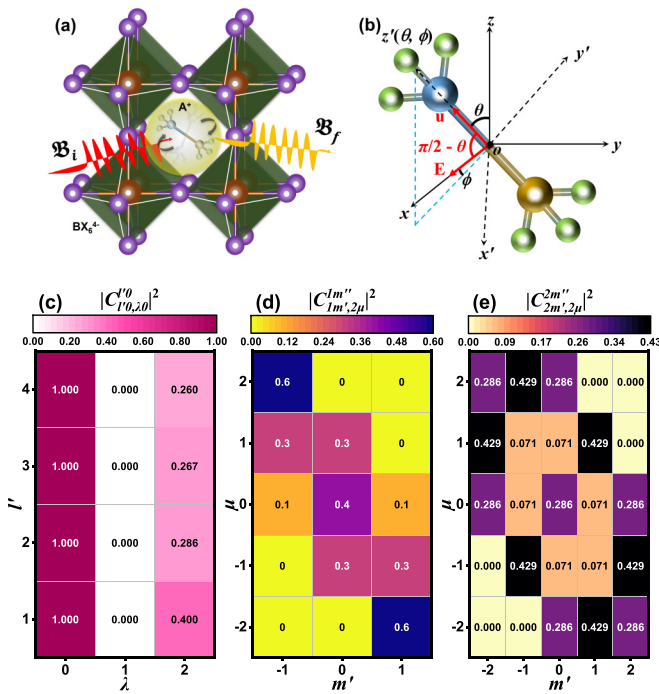


FIG. 1. (a) The schematic diagram of Raman scattering for the rotational A^+ cation in the center of BX_6^- octahedral cage, where A , B , and X correspond to the species of organic cation, metal ion, and halide anion, respectively, in MHP. \mathfrak{B}_i and \mathfrak{B}_f represent the angular momenta (in the unit of rotational constant B) of the incident and scattering photon, respectively. (b) The direction of the organic cation in the laboratory frame (x, y, z) and molecular frame (x', y', z') . (θ, ϕ) denotes the angular coordinates of organic cation in the laboratory frame. \mathbf{u} is the molecular dipole moment and \mathbf{E} is the electric field vector of the light. (c)–(e) Clebsch-Gordan coefficients for different orbital quantum states $|L = l', M = m'\rangle$, coupling with phonon angular momentum states $|\lambda, \mu\rangle$.

exciton [31–33], Raman scattering for ROC in MHP could be divided into three steps as demonstrated in Fig. 1(a): (i) the angular momentum transfer of an incident photon \mathfrak{B}_i excites the ROC from the initial state $|i\rangle = |L = l, M = m\rangle$ to $|j\rangle = |L = l', M = m'\rangle$, where these rotational eigenstates are labeled by the orbital angular number L and its projection M on the laboratory-frame z -axis, with eigenenergies $E_L = BL(L + 1)$ [34,35], B is the rotational constant; (ii) the transition from $|j\rangle = |L = l', M = m'\rangle$ to $|k\rangle = |L = l'', M = m''\rangle$ is accompanied by the exchange of angular momentum between ROC and phonons; (iii) the ROC from $|k\rangle$ comes back into the initial $|i\rangle$ with the help of the angular momentum transfer \mathfrak{B}_f by the scattering of a photon. So the cross section of Raman scattering for the ROC can be expressed as [31–33]

$$|\text{Re}|^2 = \left| \frac{\sum_{jk} \langle i | \hat{H}_{\text{opt}} | j \rangle \langle j | \hat{H}_{\text{ph}} | k \rangle \langle k | \hat{H}_{\text{opt}} | i \rangle}{[\mathfrak{B}_i - (E_j - E_i) - i\Gamma][\mathfrak{B}_i - \mathfrak{B}_f \pm E_0 - i\Gamma]} \right|^2, \quad (1)$$

where E_i (E_j) is the eigenenergy of the rotational state $|i\rangle$ ($|j\rangle$), E_0 is the rotational energy provided by phonons in units of B , and Γ is the homogeneous linewidth for the quantum

transition. $\langle i | \hat{H}_{\text{opt}} | j \rangle$ ($\langle k | \hat{H}_{\text{opt}} | i \rangle$) and $\langle j | \hat{H}_{\text{ph}} | k \rangle$ are the matrix elements for transitions between different rotational states, arising from the ROC-photon and -phonon interaction, respectively. They are key components to study the Raman scattering of ROC in the following.

For the sake of clarity, the ROC, such as CH_3NH_3^+ in MHP, is regarded as a linear molecule with frozen transitional motion. In the dipole approximation, the Hamiltonian for a ROC subjected to a linearly polarized light is given by $\hat{H}_{\text{opt}} = -\mathbf{u} \cdot \mathbf{E}$, where \mathbf{u} is the inherent dipole moment for ROC oriented along the z' -axis in the molecular frame and \mathbf{E} is the electric field vector of the light along the x -axis in the laboratory frame [36–38], while the relative orientation of these two frames is given by the Euler angle (ϕ, θ) as shown in Fig. 1(b). The ROC-light interaction is, in general, regarded as the perturbation to the system and gives rise to quantum transitions between different rotational states. After a series of mathematical processes [39], the corresponding matrix element between the $|i\rangle$ and $|j\rangle$ states is expressed as

$$\begin{aligned} \langle i | \hat{H}_{\text{opt}} | j \rangle &= F(l, l', m, m') \\ &= -uE a_{l'-1, m'} \delta_{l, l'-1} \delta_{m, m'} \\ &\quad + uE b_{l'-1, m'-1} \delta_{l, l'-1} \delta_{m, m'-1} \\ &\quad - uE b_{l-1, -(m'+1)} \delta_{l, l'-1} \delta_{m, m'+1}, \end{aligned} \quad (2)$$

where $a_{l, m}$ and $b_{l, m}$ are angular-momentum-dependent coefficients, shown in the Supplemental Material [39]. The constants u and E represent the magnitude of \mathbf{u} and \mathbf{E} . From Eq. (2), it can be inferred that the angular momentum of the incident photon results in the transition between orbital quantum states following the selection rule of $l' - l = 1$ along with the exchange of the angular momentum projection $m' - m = 0, \pm 1$ in step (i) of Raman scattering. Similarly, the emission of the photon in step (iii) satisfies the selection rule of $l - l'' = 1$ along with $m - m'' = 0, \pm 1$.

In the frame of the *angulon* model, the effective Hamiltonian describing the interaction between a ROC and phonon bath in the spherical basis is given by [28,40–42]

$$\hat{H}_{\text{ph}} = \sum_{q\lambda\mu} V_\lambda(q) [\hat{Y}_{\lambda\mu}^*(\hat{\theta}, \hat{\phi}) \hat{b}_{q\lambda\mu}^\dagger + \hat{Y}_{\lambda\mu}(\hat{\theta}, \hat{\phi}) \hat{b}_{q\lambda\mu}]. \quad (3)$$

Here $q = |\mathbf{q}|$ is the scalar representation of the phonon wave vector, satisfying the relation $\sum_q \equiv \int dq$. λ and μ define, respectively, the phonon angular momentum and its projection onto the z -axis. $\hat{Y}_{\lambda\mu}(\hat{\theta}, \hat{\phi})$ are the spherical harmonic operators, which are essential for the microscopic description of the transfer of phonon angular momentum. $\hat{b}_{q\lambda\mu}^\dagger$ and $\hat{b}_{q\lambda\mu}$ are the creation and annihilation operators of phonons in the angular momentum representation, respectively (see Refs. [28,40,43–45] for a detailed derivation). The angular-momentum-dependent interaction potential $V_\lambda(q) = v_\lambda [8\alpha_c q^2 / (2\lambda + 1)]^{1/2} \int dr r^2 f_\lambda(r) j_\lambda(qr)$ is employed for an organic cation rotating in the cage-like phonon bath, where α_c is the Fröhlich coupling constant, meaning that the exchange of the angular momentum between longitudinal optical (LO) phonons and ROC are mainly taken into account [40–42] because the LO phonon is the dominate mode caused by the lattice distortion of the cage-like structure both in the theoretical and experimental perspectives [46–49]; $j_\lambda(qr)$ is the

spherical Bessel function; v_λ and $f_\lambda(r)$ represent the strength and the shape of the potential in the respective angular momentum channel λ . Specifically, the last function describes the microscopic details of the two-body interaction between the ROC and phonon bath whose expression is proposed as [50,51]

$$f_\lambda(r) = \begin{cases} \left(\frac{r}{R}\right)^\lambda, & (r \leq R), \\ 0, & (r > R), \end{cases} \quad (4)$$

and the octahedral inorganic cage is approximated by the spherical cavity, based on the facts that (i) the rotating behavior of the organic cation in this cage was demonstrated widely by recent experiments [20,21,52,53] and (ii) the strongest coupling strength (the potential distribution) is around the spherical boundary between the ROC and inorganic cage [54,55]. $R = a_0/2$ is the effective radius of this spherical space (a_0 is the length of the side of the octahedral cage). After the proceeding some algebraic calculation, the matrix element for the transfer of the phonon angular momentum between two different rotational states is given as

$$\langle j|\hat{H}_{\text{ph}}|k\rangle = \sum_q V_\lambda(q) g_1 C_{l'0,\lambda 0}^{l''0} C_{l'm',\lambda\mu}^{l''m'}, \quad (5)$$

where $g_1 = \{(2l'+1)(2\lambda+1)/[4\pi(2l''+1)]\}^{1/2}$ and $C_{l'm',\lambda\mu}^{l''m'}$ is the Clebsch-Gordan (C-G) coefficients [56]. Eventually, upon substitution of Eqs. (2) and (5), the cross section of Raman scattering is converted into

$$|\text{Re}|^2 = \left| \frac{u^2 E^2 g_1 g_2 \sum_q V_\lambda(q) C_{l'0,\lambda 0}^{l''0} C_{l'm',\lambda\mu}^{l''m'}}{[\mathfrak{B}_i - \mathfrak{B}_f \pm E_0]^2 + \Gamma^2} \right|. \quad (6)$$

$g_2 = F(l', m, m')F(l'', l, m'', m)$ summarizes the roles of angular momentum transfer between the ROC and photon in the absorption and emission processes, ensuring the classical process of Raman scattering; namely, the initial and final states are the same one. The redistribution of angular momentum between the ROC and phonon bath in the mediated process is determined by the C-G coefficients $C_{l'0,\lambda 0}^{l''0}$ and $C_{l'm',\lambda\mu}^{l''m'}$.

III. RESULTS AND DISCUSSION

The values of $|C_{l'0,\lambda 0}^{l''0}|^2$ as functions of l' and λ are shown in Fig. 1(c), in which $l'' = l'$ is assumed, implying the orbital angular quantum is unchanged during the angular momentum exchange between the ROC and phonon. Thus, the phonon angular momentum only induces the change of the projection of orbital angular momentum, that is, the variation of the orientation of ROC. This results in the distribution of the allowed transitions (red) as well as the forbidden ones (white) depending on the phonon angular-momentum of quantum state λ , satisfying the following selection rule of $l' + l' + \lambda = \text{even}$. As a result, the lowest order of the phonon angular-momentum that dominates the transfer of angular momentum between the ROC and phonon is the quantum number $\lambda = 2$ shown in Fig. 1(c). Figures 1(d) and 1(e) present the phonon angular-momentum state $\lambda = 2$, which induces a possible transition between the projections of angular momentum reflected by C-G coefficients $|C_{1m',\lambda\mu}^{1m''}|^2$ and $|C_{2m',\lambda\mu}^{2m''}|^2$ for angular quan-

tum numbers $l' = 1$ and $l' = 2$, respectively. Two obvious features are shown that (1) the distribution of the coefficients reveals the symmetrical relations, represented as $|C_{l'm',\lambda\mu}^{l''m''}|^2 = |C_{l'-m',\lambda-\mu}^{l''-m''}|^2$; (2) the ROC is inclined to couple with phonons that can invert its angular-momentum projection from m' to $-m'$. These results indicate that ROC has the preferential directions induced by phonon angular momentum.

To give a comprehensive comparison between different transfers of phonon angular momentum, the Raman spectra for three lowest rotational levels are illustrated in Fig. 2. Here, the typical example of MHP $\text{CH}_3\text{NH}_3\text{PbI}_3$ in the cubic phase is selected in which organic cation CH_3NH_3^+ rotating in the PbI_6^{4-} octahedral cage as shown in Fig. 1(a). The values for the related parameters in Eq. (6) are listed in Table S1 in the Supplemental Material [39] (see also Refs. [57,58] and references therein). These specific values of angular-momentum-dependent coefficients $a_{l,m}$, $b_{l,m}$, and the C-G coefficients involved in the angular momenta transfer among the three lowest rotational levels are listed in Tables S3 and Table S4 [39].

First, Fig. 2(a) illustrates the Raman scattering from the ground state of ROC ($L = 0$) to the first-excited state ($L = 1$) as well as from $L = 1$ to the second-excited state ($L = 2$) with the change of the projection of angular momentum $\Delta M = \pm 1$. One can see that the Stokes process of $(L = 0, M = 0) \rightarrow (L = 1, M = 1) \rightarrow (L = 1, M = 0) \rightarrow (L = 0, M = 0)$ (\rightarrow and $\rightarrow\rightarrow$ denote the transfer of angular momentum of photon and phonon, respectively), and anti-Stokes process of $(L = 0, M = 0) \rightarrow (L = 1, M = -1) \rightarrow (L = 1, M = 0) \rightarrow (L = 0, M = 0)$ follow a symmetrical distribution with the same intensity, which can be attributed to the symmetrical relations of the C-G coefficient, shown in Fig. 1(d), and the optical coefficients given in Eq. (2). In 2015, Schmidt and Lemeshko proposed that the phonon angular momentum couples with the rotating quantum molecule (or impurity) to form a new quasiparticle—*angulon*—for the first time [28]. They pointed out that this angulon induces a rich rotational fine-structure in the spectra of molecules, such as “rotational Lamb shift.” Subsequently, they further revealed that the spectral function of the rotational molecule suddenly acquires the transfer of one quantum of phonon angular momentum from the many-body environment at a critical rotational speed; however, the direct identification for the phonon angular momentum and its transfer is still a challenging task in experiments. For Raman scattering in Fig. 2, not only is the phonon angular momentum arising from the octahedral-cage structure proved, but also its specific values could be reflected directly by the Stokes and anti-Stokes shifts. In Fig. 2(a), the Stokes process of $(L = 1, M = 0) \rightarrow (L = 2, M = 1) \rightarrow (L = 2, M = 0) \rightarrow (L = 1, M = 0)$ and the anti-Stokes process of $(L = 1, M = 0) \rightarrow (L = 2, M = -1) \rightarrow (L = 2, M = 0) \rightarrow (L = 1, M = 0)$ show similar behaviors, however, with smaller intensity owing to the different values between $C_{1m',2\mu}^{1m''}$ and $C_{2m',2\mu}^{2m''}$ given in Figs. 1(d) and 1(e), respectively. But the intensity of the Stokes process $(L = 1, M = 1) \rightarrow (L = 2, M = 2) \rightarrow (L = 2, M = 1) \rightarrow (L = 1, M = 1)$ is much stronger than that of the anti-Stokes process $(L = 1, M = 1) \rightarrow (L = 2, M = 0) \rightarrow (L = 2, M = 1) \rightarrow (L = 1, M = 1)$. Following the rules of C-G coefficients in Fig. 1(e), the asymmetrical

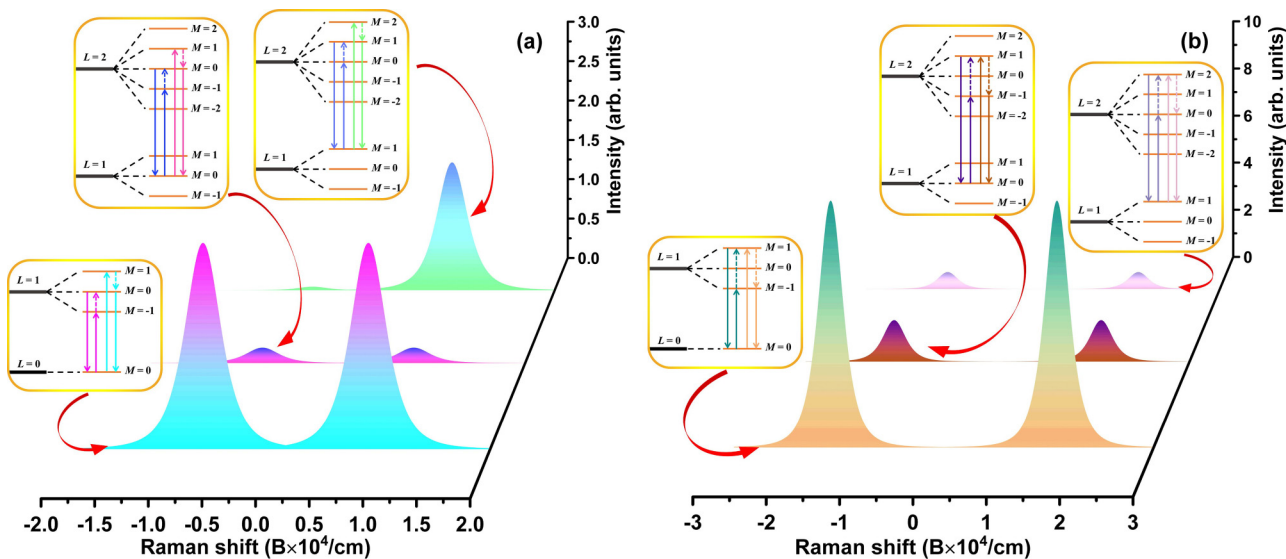


FIG. 2. The Stokes and anti-Stokes Raman scattering for three lowest rotational levels coupling with the phonon angular momentum states (a) $|\lambda = 2, \mu = \pm 1\rangle$ and (b) $|\lambda = 2, \mu = \pm 2\rangle$, respectively. The scenarios of the angular momentum transfer for different Raman processes are shown in the insets, where L and M represent the quantum number of angular momentum and its projection onto the z -axis, respectively. The rotational constant B is usually in the range of GHz–THz, corresponding to the Raman shift in the range of 0.01 – 100 cm^{-1} [28,59].

intensity distribution should also appear for these scattering processes starting from the initial states ($L = 1, M = -1$) (see Fig. S2 in the Supplemental Material [39]). From these comparisons we can infer that the difference of the initial states between ($L = 1, M = 0$) and ($L = 1, M = \pm 1$), that is, the differently initial orientation of ROC, determines the features of Raman spectra. In turn, the initial orientation of ROC (or molecules) could be reflected by Raman spectra in experiments. In fact, a series of strategies to control the alignment and orientation of the rotational molecules were proposed in past decades, such as the linearly polarized ultrafast laser pulses [60–62], two-color and static fields [63], as well as two-color femtosecond lasers and terahertz field [64,65]. The molecular alignment and orientation are crucial for a variety of applications ranging from chemical reaction dynamics to the design of molecular devices. For these applications, however, one of the most important prerequisites is to judge the initial orientation of the rotational molecules. Obviously, on the one hand, the Raman scattering of the rotational molecule provides an effective method to overcome this issue. On the other hand, the detailed dynamics and some novel physical phenomena related to the rotational particles in the many-body bath should be analyzed deeply by Raman scattering even though the rotational structure and dynamics of molecules were obtained widely from infrared spectroscopy [66,67].

Figure 2(b) shows Raman scattering starting from the ground and first-excited states of ROC with the change of projection of angular momentum $\Delta M = \pm 2$. One can see that the Stokes and anti-Stokes scattering starting from the initial states ($L = 0, M = 0$) and ($L = 1, M = 0$) have the same intensity. Moreover, the magnitude is much stronger than the corresponding scattering shown in Fig. 2(a). This indicates the rotation of the organic cation has the preferential orientation at a certain external condition, which is very consistent with

the prediction of the C-G coefficient in Fig. 1(e). Therefore, this kind of Raman scattering would provide the anticipation for these chemical reactions depending on the high-precision control of the spatial orientation of the molecules, e.g., molecular imaging and selectivity [68], the enhancement of the interaction of a molecule with a surface in the precise catalytic process [69,70]. For Raman scattering starting from the same states ($L = 1, M = \pm 1$) of the ROC in Figs. 2(a) and 2(b), the spectral shapes show a significant difference since the change of projection of angular momentum follows $\Delta M = \pm 1$ and $\Delta M = \pm 2$, respectively. This means that the variational magnitude of the orientation of a ROC could be estimated by the spectral shape, which suggests the possibility to judge and modulate a molecule from a well-defined initial state to a target state.

The phonon angular momentum not only induces the variation of orientation of ROC at a given orbital quantum state, but induces transitions between different orbital states in Raman scattering when the second-order term of the photon interacting with ROC is considered. We illustrate the processes of $(L = 0, M = 0) \rightarrow (L = 2, M = 0) \rightarrow (L = 1, M = 0) \rightarrow (L = 0, M = 0)$ and $(L = 0, M = 0) \rightarrow (L = 1, M = 0) \rightarrow (L = 2, M = 0) \rightarrow (L = 0, M = 0)$ without the variation of orientation as well as the processes of $(L = 0, M = 0) \rightarrow (L = 2, M = 0) \rightarrow (L = 1, M = -1) \rightarrow (L = 0, M = 0)$ and $(L = 0, M = 0) \rightarrow (L = 1, M = -1) \rightarrow (L = 2, M = 0) \rightarrow (L = 0, M = 0)$ with the change of orientation $\Delta M = \pm 1$ in Fig. S3 [39]. One can see that these scatterings have similar features with the processes in Fig. 2, but the intensity becomes weaker by nearly one order of magnitude, demanding more accurate detection techniques. In fact, these scattering behaviors for the three lowest rotational levels can be generalized to more quantum transitions between rotational levels assisted by photon and phonon angular momenta for ROC in MHP and could be

explored by Raman scattering. Therefore, this type of Raman scattering could get deeply into more complicated quantum transitions and reveal the fine spectroscopy of the rotational systems. Besides the rotational molecules or impurities as intermediaries for the Raman scattering, other elementary excitations in physics, such as the interlayer and intralayer excitons in van der Waals heterostructures [71,72], should have similar Raman scattering when the rotational degree of freedom is considered. Lastly, we must emphasize that (1) only the angular momentum of the LO phonon is considered in this study, other phonon modes have a similar effect and will play an important role at a certain condition; (2) the perovskite materials undergo two structure phase transitions with temperature, the influence of which on the coupling strength between phonon bath and ROC, as well as the shape of the potential are also significant [73]. These effects are out of the scope of this study.

In summary, we develop a microscopic theory to describe the Raman scattering of an organic cation rotating in the octahedral cage of MHP. This theory predicts that the Raman spectra provide an effective and direct method to reflect the transfer of phonon angular momentum and its specific values in the many-body environment. Meanwhile, two key prerequisites for the alignment and orientation of the rotational molecules could be judged by Raman spectra, which may open a new door to explore quantum control of particle rotation in many-body physics.

ACKNOWLEDGMENTS

This work was supported by National Natural Science Foundation of China (Grants No. 11674241 and No. 12174283).

-
- [1] M. A. Green, A. Ho-Baillie, and H. J. Snaith, *Nat. Photonics* **8**, 506 (2014).
- [2] S. A. Veldhuis, P. P. Boix, N. Yantara, M. Li, T. C. Sum, N. Mathews, and S. G. Mhaisalkar, *Adv. Mater.* **28**, 6804 (2016).
- [3] W. Tian, H. Zhou, and L. Li, *Small* **13**, 1702107 (2017).
- [4] A. Filippetti and A. Mattoni, *Phys. Rev. B* **89**, 125203 (2014).
- [5] J. Y. Kim, J.-W. Lee, H. S. Jung, H. Shin, and N.-G. Park, *Chem. Rev.* **120**, 7867 (2020).
- [6] A. A. Bakulin, O. Selig, H. J. Bakker, Y. L. Rezus, C. Müller, T. Glaser, R. Lovrincic, Z. Sun, Z. Chen, A. Walsh, J. M. Frost, and T. L. C. Jansen, *J. Phys. Chem. Lett.* **6**, 3663 (2015).
- [7] Y. Guo, O. Yaffe, D. W. Paley, A. N. Beecher, T. D. Hull, G. Szpak, J. S. Owen, L. E. Brus, and M. A. Pimenta, *Phys. Rev. Mater.* **1**, 042401(R) (2017).
- [8] W. M. J. Franssen, S. G. D. van Es, R. Dervisoglu, G. A. de Wijs, and A. P. M. Kentgens, *J. Phys. Chem. Lett.* **8**, 61 (2017).
- [9] J. S. Bechtel, R. Seshadri, and A. Van der Ven, *J. Phys. Chem. C* **120**, 12403 (2016).
- [10] J.-H. Lee, N. C. Bristowe, J. H. Lee, S.-H. Lee, P. D. Bristowe, A. K. Cheetham, and H. M. Jang, *Chem. Mater.* **28**, 4259 (2016).
- [11] J. H. Lee, J.-H. Lee, E.-H. Kong, and H. M. Jang, *Sci. Rep.* **6**, 21687 (2016).
- [12] J. Kang and L.-W. Wang, *J. Phys. Chem. Lett.* **8**, 3875 (2017).
- [13] J.-W. Lee, S. Tan, S. I. Seok, Y. Yang, and N.-G. Park, *Science* **375**, eabj1186 (2022).
- [14] J. M. Frost, K. T. Butler, F. Brivio, C. H. Hendon, M. van Schilfgaarde, and A. Walsh, *Nano Lett.* **14**, 2584 (2014).
- [15] C. Goehry, G. A. Nemnes, and A. Manolescu, *J. Phys. Chem. C* **119**, 19674 (2015).
- [16] S. Meloni, T. Moehl, W. Tress, M. Franckevicius, M. Saliba, Y. H. Lee, P. Gao, M. K. Nazeeruddin, S. M. Zakeeruddin, U. Rothlisberger, and M. Graetzel, *Nat. Commun.* **7**, 10334 (2016).
- [17] B. Kim, J. Kim, and N. Park, *Sci. Rep.* **10**, 19635 (2020).
- [18] G. M. Koutentakis, A. Ghazaryan, and M. Lemeshko, *arXiv:2301.09875*.
- [19] I. P. Swainson, C. Stock, S. F. Parker, L. Van Eijck, M. Russina, and J. W. Taylor, *Phys. Rev. B* **92**, 100303(R) (2015).
- [20] A. M. A. Leguy, J. M. Frost, A. P. McMahon, V. G. Sakai, W. Kockelmann, C. Law, X. Li, F. Foglia, A. Walsh, B. C. O'Regan, J. Nelson, J. T. Cabral, and P. R. F. Barnes, *Nat. Commun.* **6**, 7124 (2015).
- [21] B. Li, Y. Kawakita, Y. Liu, M. Wang, M. Matsuura, K. Shibata, S. Ohira-Kawamura, T. Yamada, S. Lin, K. Nakajima, and S. Liu, *Nat. Commun.* **8**, 16086 (2017).
- [22] C. P. Koch, M. Lemeshko, and D. Sugny, *Rev. Mod. Phys.* **91**, 035005 (2019).
- [23] Y. Shagam, A. Klein, W. Skomorowski, R. Yun, V. Averbukh, C. P. Koch, and E. Narevicius, *Nat. Chem.* **7**, 921 (2015).
- [24] K. Chordiya, I. Simkó, T. Szidarovszky, and M. U. Kahaly, *Sci. Rep.* **12**, 8280 (2022).
- [25] D. Mitra, K. H. Leung, and T. Zelevinsky, *Phys. Rev. A* **105**, 040101 (2022).
- [26] K. L. Svane, A. C. Forse, C. P. Grey, G. Kieslich, A. K. Cheetham, A. Walsh, and K. T. Butler, *J. Phys. Chem. Lett.* **8**, 6154 (2017).
- [27] W. Xu, Q. Hu, S. Bai, C. Bao, Y. Miao, Z. Yuan, T. Borzda, A. J. Barker, E. Tyukalova, Z. Hu, M. Kawecki, H. Wang, Z. Yan, X. Liu, X. Shi, K. Uvdal, M. Fahlman, W. Zhang, M. Duchamp, J.-M. Liu, A. Petrozza, J. Wang, L.-M. Liu, W. Huang, and F. Gao, *Nat. Photonics* **13**, 418 (2019).
- [28] R. Schmidt and M. Lemeshko, *Phys. Rev. Lett.* **114**, 203001 (2015).
- [29] J. P. Toennies and A. F. Vilesov, *Angew. Chem. Int. Ed.* **43**, 2622 (2004).
- [30] J. B. Balewski, A. T. Krupp, A. Gaj, D. Peter, H. P. Buchler, R. Low, S. Hofferberth, and T. Pfau, *Nature (London)* **502**, 664 (2013).
- [31] B. Zhu, K. Huang, and H. Tang, *Phys. Rev. B* **40**, 6299 (1989).
- [32] H. Tang, B. Zhu, and K. Huang, *Phys. Rev. B* **42**, 3082 (1990).
- [33] Z.-W. Wang, Y. Xiao, J.-P. Deng, Y. Cui, and Z.-Q. Li, *Phys. Rev. B* **100**, 125308 (2019).
- [34] H. Lefebvre-Brion and R. W. Field, *The Spectra and Dynamics of Diatomic Molecules* (Elsevier, New York, 2004).
- [35] P. F. Bernath, *Spectra of Atoms and Molecules*, 2nd ed. (Oxford, New York, 2005).
- [36] R. N. Zare, *Angular Momentum: Understanding Spatial Aspects in Chemistry and Physics* (Wiley, New York, 1988).

- [37] C. M. Dion, A. Keller, O. Atabek, and A. D. Bandrauk, *Phys. Rev. A* **59**, 1382 (1999).
- [38] R. R. Riso, T. S. Haugland, E. Ronca, and H. Koch, *Nat. Commun.* **13**, 1368 (2022).
- [39] See Supplemental Material at <http://link.aps.org/supplemental/10.1103/PhysRevB.107.094306> for details on the ROC-light and -phonon coupling, the values of C-G coefficients and Raman spectra for three lowest rotational levels.
- [40] R. Schmidt and M. Leshko, *Phys. Rev. X* **6**, 011012 (2016).
- [41] M. Leshko, *Phys. Rev. Lett.* **118**, 095301 (2017).
- [42] E. Yakaboylu, B. Midya, A. Deuchert, N. Leopold, and M. Leshko, *Phys. Rev. B* **98**, 224506 (2018).
- [43] M. Leshko, R. V. Krems, J. M. Doyle, and S. Kais, *Mol. Phys.* **111**, 1648 (2013).
- [44] X. Li, R. Seiringer, and M. Leshko, *Phys. Rev. A* **95**, 033608 (2017).
- [45] M. Leshko and R. Schmidt, in *Low Energy and Low Temperature Molecular Scattering*, edited by A. Osterwalder and O. Dulieu (RSC, London, 2017).
- [46] C. Quarti, G. Grancini, E. Mosconi, P. Bruno, J. M. Ball, M. M. Lee, H. J. Snaith, A. Petrozza, and F. D. Angelis, *J. Phys. Chem. Lett.* **5**, 279 (2014).
- [47] F. Brivio, J. M. Frost, J. M. Skelton, A. J. Jackson, O. J. Weber, M. T. Weller, A. R. Goni, A. M. A. Leguy, P. R. F. Barnes, and A. Walsh, *Phys. Rev. B* **92**, 144308 (2015).
- [48] C. M. Iaru, J. J. Geuchies, P. M. Koenraad, D. Vanmaekelbergh, and A. Y. Silov, *ACS Nano* **11**, 11024 (2017).
- [49] C. M. Iaru, A. Brodu, N. J. J. van Hoof, S. E. T. ter Huurne, J. Buhot, F. Montanarella, S. Buhbut, P. C. M. Christianen, D. Vanmaekelbergh, C. de M. Donega, J. G. Rivas, P. M. Koenraad, and A. Y. Silov, *Nat. Commun.* **12**, 5844 (2021).
- [50] K. Oshiro, K. Akai, and M. Matsuura, *Phys. Rev. B* **58**, 7986 (1998).
- [51] A. Alexandrescu, D. Cojoc, and E. Di Fabrizio, *Phys. Rev. Lett.* **96**, 243001 (2006).
- [52] S. Kanno, Y. Imamura, A. Saeki, and M. Hada, *J. Phys. Chem. C* **121**, 14051 (2017).
- [53] O. Selig, A. Sadhanala, C. Müller, R. Lovrincic, Z. Chen, Y. L. A. Rezus, J. M. Frost, T. L. C. Jansen, and A. A. Bakulin, *J. Am. Chem. Soc.* **139**, 4068 (2017).
- [54] S. Kanno, Y. Imamura, and M. Hada, *J. Phys. Chem. C* **122**, 15966 (2018).
- [55] P. R. Varadwaj, A. Varadwaj, H. M. Marques, and K. Yamashita, *Sci. Rep.* **9**, 50 (2019).
- [56] D. A. Varshalovich, A. N. Moskalev, and V. K. Khersonski, *Quantum Theory of Angular Momentum* (World Scientific, Singapore, 1988).
- [57] P. W. Fowler and M. L. Klein, *J. Chem. Phys.* **85**, 3913 (1986).
- [58] T. Kirchartz, T. Markvart, U. Rau, and D. A. Egger, *J. Phys. Chem. Lett.* **9**, 939 (2018).
- [59] J. A. Davies, C. Schran, F. Briec, D. Marx, and A. M. Ellis, *Phys. Rev. Lett.* **130**, 083001 (2023).
- [60] R. Baumfalk, N. H. Nahler, and U. Buck, *J. Chem. Phys.* **114**, 4755 (2001).
- [61] I. Sh. Averbukh and R. Arvieu, *Phys. Rev. Lett.* **87**, 163601 (2001).
- [62] H. Stapelfeldt and T. Seideman, *Rev. Mod. Phys.* **75**, 543 (2003).
- [63] T. Kanai and H. Sakai, *J. Chem. Phys.* **115**, 5492 (2001).
- [64] S. De, I. Znakovskaya, D. Ray, F. Anis, N. G. Johnson, I. A. Bocharova, M. Magrakvelidze, B. D. Esry, C. L. Cocke, I. V. Litvinyuk, and M. F. Kling, *Phys. Rev. Lett.* **103**, 153002 (2009).
- [65] C.-C. Shu and N. E. Henriksen, *Phys. Rev. A* **87**, 013408 (2013).
- [66] S. Grebenev, M. Hartmann, M. Havenith, B. Sartakov, J. P. Toennies, and A. F. Vilesov, *J. Chem. Phys.* **112**, 4485 (2000).
- [67] M. Y. Choi, G. E. Douberly, T. M. Falconer, W. K. Lewis, C. M. Lindsay, J. M. Merritt, P. L. Stiles, and R. E. Miller, *Int. Rev. Phys. Chem.* **25**, 15 (2006).
- [68] A.-T. Le, R. R. Lucchese, M. T. Lee, and C. D. Lin, *Phys. Rev. Lett.* **102**, 203001 (2009).
- [69] S. Li, A. Yu, F. Toledo, Z. Han, H. Wang, H. Y. He, R. Wu, and W. Ho, *Phys. Rev. Lett.* **111**, 146102 (2013).
- [70] A. Shiotari, S. E. M. Putra, Y. Shiozawa, Y. Hamamoto, K. Inagaki, Y. Morikawa, Y. Sugimoto, J. Yoshinobu, and I. Hamada, *Small* **17**, 2008010 (2021).
- [71] E. Torun, H. P. C. Miranda, A. Molina-Sánchez, and L. Wirtz, *Phys. Rev. B* **97**, 245427 (2018).
- [72] X. Lu, X. Li, and L. Yang, *Phys. Rev. B* **100**, 155416 (2019).
- [73] M. Keshavarz, M. Ottesen, S. Wiedmann, M. Wharmby, R. Küchler, H. Yuan, E. Debroye, J. A. Steele, J. Martens, N. E. Hussey, M. Bremholm, M. B. J. Roefsaers, and J. Hofkens, *Adv. Mater.* **31**, 1900521 (2019).